JJEE
Volume 9 | Number 2 | June 2023 | Pages 209-227

Jordan Journal of Electrical Engineering

ISSN (print): 2409-9600, ISSN (online): 2409-9619

Homepage: jjee.ttu.edu.jo

Investigation of Voltage Dip Problems during Faults on a Grid-Tied Doubly Fed Induction Generator in a Wind Energy System

Milkias Berhanu Tuka*

Electrical Power and Control Engineering Department, Adama Science and Technology University, Adama, Ethiopia
E-mail: mil_ber2000@astu.edu.et

Received: November 21, 2022 *Revised: December 24, 2022* *Accepted: January 01, 2023*

Abstract – A voltage dip is a sudden drop of voltages - generally between 10 and 90 % of the rated RMS value - during a period lasting from half a cycle to a few seconds on the phases of the power lines. It is one of the most important power quality problems affecting the stability of the Doubly Fed Induction Generator (DFIG) in Wind Energy Conversion System (WECS) and hence needs to be analyzed for a given machine for its performance analysis under grid disturbances. When a voltage dip problem happens in the given power as of faults, the magnitude of the rotor and stator currents of DFIG get increased, and hence disturbs steady state operation of the system. Therefore, in this paper, the worst voltage dip of 90 % is tested for grid faults on a 5 kW DFIG to validate its performance under this phenomenon. Based on the results of the simulation - along with its experimental validation - the machine is found to be robust for faults staying a shorter period without disconnecting it from the grid. On the other hand, operating a machine for a longer period while keeping it connected to a grid during a heavy dip, may result in its degradation as the rated limits are violated. To rectify and mitigate the aforesaid problems, a control system - with and without a crowbar - is developed for symmetrical faults to tackle such a problematic situation, and to discuss its fulfillment of the current grid code requirements. Finally, a complete model of the DFIG coupled with the grid is developed, modeled, analyzed and simulated using MATLAB/Simulink user-defined function toolbox block.

Keywords – Control system; Doubly fed induction generator; Modelling; Symmetrical faults; Voltage dips.

1. INTRODUCTION

Voltage dip is defined in EN50160 as a temporary reduction of the RMS voltage at a common point of the electrical supply system to a value below 90% of rated voltage followed by a voltage recovery after 10 ms to 1 minute [1, 2].

According to IEEE-1159 and IEC definitions, these include variations in the fundamental frequency voltage that last less than one minute by best characterized on plots of the RMS voltage versus time. But it is often enough to describe them by a voltage magnitude and a duration that the voltage is outside of specified thresholds [3] as used in this paper.

All electrical drives connected to a grid are affected to a greater or lesser degree by voltage dips. Three-phase voltages can become unbalanced and distorted because of the effect of nonlinear loads, transient grid faults, unpredicted short circuits, intentional changing of a power system configuration, transformers energization, and connection of large induction motors.

* Corresponding author
Article's DOI: 10.5455/jjee.204-1669028936

Considering dynamic changes in the power quality requirements and the development of power electronics devices, it is worth enough to focus on the control methods of power electronic converters and their reliability in case of grid voltage dips, higher harmonics, etc. to a system optimal and stable at least with intolerable range.

One of the main advantages of the Doubly Fed Induction Generator (DFIG) is that it provides a variable speed using a small and economical power converter. These machines are controlled by a converter connected to the rotor, where the power is only a small fraction - approximately equal to the slip - of the stator power. This characteristic makes the DFIG especially suitable for applications where the slip is narrowly limited, such as wind turbines (WT) [4, 5]. However, as wind energy penetration increased and the number of wind turbines using the DFIG expanded, its main disadvantage, that is, its excessive sensitivity to electric grid disturbances becomes more and more relevant and increased [4]. Despite this fact, the DFIG-based Wind Turbines are responsible for producing 50% of installed wind power worldwide [6] by properly controlling their operating actions under voltage dip scenarios as this is the main focus of this paper.

The desired independent active and reactive power flow control in a given power system requires selecting appropriate pairs of voltage magnitude and phase angle [7]. Despite its limitations during voltage dip conditions, the DFIM has interesting features of active and reactive power control capabilities. A voltage dip causes overcurrents and overvoltages in the rotor windings, which would damage the converter connected to their terminals if no countermeasures were taken.

As industrial processes have become more automated, the equipment has become increasingly sensitive to these momentary under voltages. If a single piece of equipment in the process is affected by the voltage sag, the entire process can be interrupted. This is one of the main reasons for focusing on its control actions.

2. LITERATURE SURVEY

When a voltage dip occurs, the wind turbines in the wind farm try to disconnect from the system to protect the converters from over voltages and over currents. On the other hand, the various latest grid codes demand them to stay connected with the grid supplying power to the system even in this horrible situation. That means, they need to possess fault ride-through (FRT) capability under these conditions. For instance, the Grid Code of countries mentioned in [1, 8] states that all wind turbines must remain connected in the event of any short circuit in the high-voltage transmission network. Having this into conception, there are various types of research under investigation of the phenomenon and providing different kinds of control mechanisms that bring optimum solutions. For instance, the study described in [9] suggests improving the generator terminal voltage during a grid fault using shunt reactive power compensation. On the other side, the use of the crowbar is evaluated in [10]. The inherent difficulty of ride-through control during a symmetrical grid fault is explained in [11]. Limiting the high current in the rotor and providing a bypass for it via a set of resistors (crowbar) that are connected to the rotor circuit of a machine is provided as a proposed method of solution in [12] making wind turbines with DFIG stay connected with the grid during grid faults. Initially, the solution implemented by the manufacturers to protect the converter was to short-circuit the rotor windings with the so-called crowbar and

disconnect the turbine from the grid [13]. With this solution, the wind turbines are not able to collaborate in resuming the normal operation of the grid. Even worse they contribute to increasing the dip as they stop generating electric power. However, there lacks sufficient references and works in the area of developing detailed models, control, protection, etc. for a dip in relating it with grid code requirements of various countries. Thus, this paper tries to fill the gap by putting its contribution with proper control of active and reactive power which can analogously be considered on the other hand as another issue of power quality problem mitigation techniques.

It can again be realized that the Doubly Fed Induction Generator (DFIG) and back-to-back converter are very sensitive to power quality disturbances in grid-connected wind energy conversion systems (WECSs) with special attention for their protection from voltage sags, considering the introduction of several low-voltage ride-through (LVRT) techniques [14].

So far, the influence of wind turbines on the evolution of voltage dips has been small due to the low penetration of wind energy. However, as the number of grid-connected turbines grows, this influence has become more important.

In this study, limiting a rotor current by letting the excess current flow through a set of resistors (crowbar protection) together with control techniques in compliance with grid code requirements towards supporting it with a reactive power under a limited active power production during a voltage dip is implemented for a given machine using MATLAB-Simulink/PowerSym software and practical results have been obtained for its validation. For this reason, a programmable voltage source of the MATLAB toolbox is used to implement different kinds of voltage dips. Practical results from the previous studies [15] have offered very useful suggestions of hardware setup for different kinds of machines, yet there exists a lack of detailed explanation of a machine at a real-time simulation with a Digital Signal Processing (DSP) micro-controller-based approach that would be useful to validate for optimal results.

Many countries, especially in the developing parts of the world, have considerable wind resources that are still untapped. A key barrier in these countries is their lack of expertise, concerning both methods of site selection and technical aspects of wind power [16]. In connection, many African countries are at the infant stage of producing their power from renewable energy, especially wind power. Similarly, Ethiopia has no officially announced and developed grid codes regarding wind turbines up to very recent times [17] even though the countries installed capacity from wind reached 324 MW while 100 GW is the expected potential [18]. Thus, aiming to fill the gap and being used as a reference for further research works, this paper models a system for a given machine tied with a grid under voltage dip scenarios.

3. DYNAMIC MODELING OF DOUBLY-FED INDUCTION GENERATOR

Before proceeding to the control and analysis of the DFIG in depth for its performance, its model in space vector form using Clarke (αβ) and Park (dq) transformations is very important.

Three sets of voltage, flux linkage, and motion equations of the induction generator can be used to describe it in space-vector [20]. The most widely used vector/field-oriented

control and direct control techniques can be applied for DFIGs in wind power systems [17]. However, in this study, only a vector control technique in the form of the two-phase dq-representation under a stator flux frame of orientation is used.

3.1. Alpha-Beta (αβ) Model

By using a known Clarke and its inverse transformation, the three-phase (abc) quantities are converted into two stationary frames (αβ) quantities and vice versa. The instantaneous value of the grid voltage in αβ can be used to find out the grid voltage angle, φ_g as given in Eq. (1). If V_{ag}, V_{bg}, and V_{cg} are three-phase balanced sinusoidal waveforms of grid voltages, φ_g can then be obtained as [20]:

$$\varphi_g = \tan^{-1}\left(\frac{V_\beta}{V_\alpha}\right) \quad (1)$$

or considering all four quadrants such as:

$$\varphi_g = \text{atan2}\left(\frac{V_\beta}{V_\alpha}\right) \quad (2)$$

A diagram showing the different reference frames used in the DFIG is presented in Fig. 1 where αβ is a stator reference frame, DQ is the rotor reference frame rotating at ω_m and the dq is synchronous reference frame rotating at ω_g. Subscripts "s", "r" and "a" denotes the stator, rotor, and synchronous reference frames, respectively. Clark, Park, and their inverse transformations can be applied on a space vector to represent it on any of these frames [22].

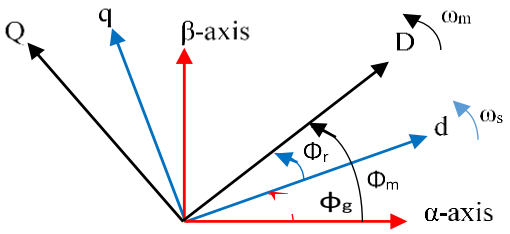

Fig. 1. An alignment of reference frames [22].

For the motor convention under 5th order modeling which includes the stator flux dynamics, the stator voltage (V_s) equations can be derived as:

$$V_S^{\,s} = I_s^{\,s}R_S + \frac{d\psi_S^{\,s}}{dt}; \qquad V_r^{\,r} = I_r^{\,r}R_r + \frac{d\psi_r^{\,r}}{dt} \quad (3)$$

The stator voltage equation can be split in its alpha and beta components as follows to yield the following set of equations [4]:

$$V_S^{\,s} = I_S^{\,s}R_S + \frac{d\psi_S^{\,s}}{dt} \Rightarrow \begin{cases} v_{\alpha s} = r_s i_{\alpha s} + \dfrac{d\psi_{\alpha s}}{dt} \\ v_{\beta s} = r_s i_{\beta s} + \dfrac{d\psi_{\beta s}}{dt} \end{cases} \quad (4)$$

where $V_{\alpha s}$, $V_{\beta s}$, $i_{\alpha s}$, $i_{\beta s}$, $i_{\alpha r}$, $i_{\beta r}$ and $\psi_{\alpha s}$, $\psi_{\beta s}$, $\psi_{\alpha r}$, $\psi_{\beta r}$ are voltages (V), currents (A) and flux linkages (wb) of the stator and rotor in αβ-axis in vector form, R_s is stator resistance.

The rotor voltage (V_r) in the stator reference frame is:

$$V_r^{\,s} = i_r^{\,s}R_r + \begin{bmatrix} 0 & 1 \\ -1 & 0 \end{bmatrix}\omega_m.\psi_r^{\,s} + \frac{d\psi_r^{\,s}}{dt} \Rightarrow \begin{cases} v_{\alpha r} = R_r i_{\alpha r} + \dfrac{d\psi_{\alpha r}}{dt} + \omega_m \psi_{\beta r} \\ v_{\beta r} = R_r i_{\beta r} + \dfrac{d\psi_{\beta r}}{dt} - \omega_m \psi_{\alpha r} \end{cases} \quad (5)$$

In the same way, the expressions for the stator and rotor fluxes in space vector form under a stationary reference frame can be obtained and given as:

$$\begin{bmatrix} \psi_s^{\,s} \\ \psi_r^{\,s} \end{bmatrix} = \begin{bmatrix} L_s & L_m \\ L_m & L_r \end{bmatrix}.\begin{bmatrix} i_s^{\,s} \\ i_r^{\,s} \end{bmatrix} \rightarrow \begin{cases} \psi_{\alpha s} = L_s i_{\alpha s} + L_m i_{\alpha r}\,; \psi_{\beta s} = L_s i_{\beta s} + L_m i_{\beta r} \\ \psi_{\alpha r} = L_m i_{\alpha s} + L_r i_{\alpha r}\,; \psi_{\beta r} = L_m i_{\beta s} + L_r i_{\beta r} \end{cases} \quad (6)$$

Solving Eq. (6) for the currents:

$$\begin{bmatrix} i_s^{\,s} \\ i_r^{\,s} \end{bmatrix} = K\begin{bmatrix} -L_r & L_m \\ L_m & -L_s \end{bmatrix}\begin{bmatrix} \psi_s^{\,s} \\ \psi_r^{\,s} \end{bmatrix} \quad (7)$$

where $K = \dfrac{1}{L_m^{\,2} - L_s.L_r}$, $L_s = L_{\sigma s} + L_m$, and $L_r = L_{\sigma r} + L_m$. R_r is rotor resistances [Ω], L_s, L_r, L_m are the stator, rotor, and mutual inductances [H]. L_{os} and L_{or} are the stator and rotor leakage inductances [H], ω is the speed of the reference frame [rad/s], ω_m is the mechanical angular velocity of the generator rotor [rad/s].

3.2. DQ Model

The space vector model of the DFIG can also be represented in a synchronously rotating frame by multiplying the voltage expressions by $e^{-j\theta s}$ and $e^{-j\theta r}$ for the stator and rotor, respectively. As a result, the dq voltage equations are [22]:

$$\vec{V}_S^{\,r} = \vec{I}_S^{\,r} R_S + \frac{d\vec{\psi}_S^{\,r}}{dt} + j\vec{\omega}_S^{\,r} \rightarrow \begin{cases} v_{ds} = R_s i_{ds} + \dfrac{d\psi_{ds}}{dt} - \omega_s \psi_{qs} \\ v_{qs} = R_s i_{qs} + \dfrac{d\psi_{qs}}{dt} + \omega_s \psi_{ds} \end{cases} \quad (8)$$

$$\vec{V}_r^{\,r} = \vec{I}_r^{\,r} R_r + \frac{d\vec{\psi}_r^{\,r}}{dt} + j\vec{\omega}_r^{\,r} \rightarrow \begin{cases} v_{dr} = R_r i_{dr} + \dfrac{d\psi_{dr}}{dt} - \omega_r \psi_{qr} \\ v_{qr} = R_r i_{qr} + \dfrac{d\psi_{qr}}{dt} + \omega_r \psi_{dr} \end{cases} \quad (9)$$

where $\omega_r = \omega_s - \omega_m$, V_{ds}, V_{qs}, i_{ds}, i_{qs}, i_{dr}, i_{qr} and ψ_{ds}, ψ_{qs}, ψ_{dr}, ψ_{qr} are voltages [V], currents [A], and flux linkages [wb] of the stator and rotor in direct (d-axis) and quadrature (q-axis) axis in vector form, P is the number of pole pairs. R_s and R_r are the stator and rotor resistances.

The relation between the mechanical speed of the shaft ω_m and the electrical speed depends on the pole pairs (p) of the machine and is given as $\omega_e = p\omega_m$ [22]. The units of these two equations are given in rad/s. The slip (s) of the machine is defined as follows:

$$s = \frac{\omega_s - \omega_m}{\omega_s} = \frac{\omega_r}{\omega_s} \rightarrow \omega_r = s.\omega_s \quad \text{and } f_r = s.f_s$$

Similarly, the fluxes yield:

$$\begin{bmatrix} \psi_s^r \\ \psi_r^r \end{bmatrix} = \begin{bmatrix} L_s & L_m \\ L_m & L_r \end{bmatrix} . \begin{bmatrix} i_s^r \\ i_r^r \end{bmatrix} \rightarrow \begin{cases} \psi_{ds} = L_s i_{ds} + L_m i_{dr} \\ \psi_{qs} = L_s i_{qs} + L_m i_{qr} \\ \psi_{dr} = L_m i_{ds} + L_r i_{qr} \\ \psi_{qr} = L_m i_{qs} + L_r i_{qr} \end{cases} \quad (10)$$

For a sinusoidal supply of voltages, at a steady state, the dq components of the voltages, currents, and fluxes will be constant values, in contrast to the αβ components that are sinusoidal magnitudes. Hence, the dq equivalent circuit model of the DFIM, in synchronous coordinates, is used.

The torque and power expressions in the dq reference frame are equivalent to the αβ equations:

$$P_s = 1.5(v_{ds} i_{ds} + v_{qs} i_{qs});$$
$$P_r = 1.5(v_{dr} i_{dr} + v_{qr} i_{qr}); \quad (11)$$
$$P_g = P_s + P_r = 1.5(v_{ds} i_{ds} + v_{qs} i_{qs} + v_{dr} i_{dr} + v_{qr} i_{qr})$$

$$Q_s = 1.5(v_{qs} i_{ds} - v_{ds} i_{qs});$$
$$Q_r = 1.5(v_{qr} i_{dr} - v_{dr} i_{qr}); \quad (12)$$
$$Q_g = Q_s + Q_r = 1.5\left[v_{qs} i_{ds} + v_{qr} i_{dr} - (v_{ds} i_{qs} + v_{dr} i_{qr}) \right]$$

$$T_{em} = 1.5p(\psi_{dr} i_{qs} - \psi_{qr} i_{ds}) = 1.5pLm(i_{dr} i_{qs} - i_{qr} i_{ds}) \quad (13)$$

where P is the number of pole pairs.

The power losses accompanied by the stator and rotor windings and saturations are neglected.

4. MODELLING DFIG UNDER VOLTAGE DIPS

The dynamic 5th order modeling of the DFIG used in the basic vector control method can be extended to incorporate transient situations due to grid disturbances. Accordingly, the whole control system for both Rotor Side Converter (RSC) and Grid Side Converter (GSC) are modified to include the negative and positive sequence components.

Stator active power (P_s), stator reactive power (Q_s), and electromechanical torque (T_{em}) expressions in the dq reference frame for DFIG under unbalanced voltage conditions are derived such as [6, 8]:

$$P_s = \frac{3}{2} \mathrm{Re}\left\{ \overrightarrow{v_s} . \overrightarrow{i_s}^* \right\} = \frac{3}{2} (v_{ds} i_{ds} + v_{qs} i_{qs}) \quad (14)$$

$$Q_s = \frac{3}{2} \mathrm{Im}\left\{ \overrightarrow{v_s} . \overrightarrow{i_s}^* \right\} = \frac{3}{2} (v_{qs} i_{ds} - v_{ds} i_{qs}) \quad (15)$$

$$T_{em} = \frac{3}{2} p \frac{L_m}{L_s} \mathrm{Im}\left\{ \overrightarrow{\psi_s} . \overrightarrow{i_r}^* \right\} = \frac{3}{2} p \frac{L_m}{L_s} (\psi_{qs} i_{dr} - \psi_{ds} i_{qr}) \quad (16)$$

The fifth order differential equation that describes the wind turbine drive system by a one-mass model taking the mechanical load torque (T_m) applied to the shaft as developed by wind speed variations to describe the dynamic motion is given as [23, 24]:

$$T_{em} - T_m = J\frac{d\omega_m}{dt} \quad (17)$$

where J is the total moment of inertia (kg.m²)

Using the expression of these powers given in Eqs. (14) and (15) and splitting them into the positive and the negative sequences, we can have [4, 22, 25]:

$$P_s = \frac{3}{2}\mathrm{Re}\left\{\vec{v_s}.\vec{i_s}^{*}\right\} = 3\mathrm{Re}\left\{(V_1e^{j\omega_s t} + V_2e^{-j\omega_s t}).(I_{s1}e^{j\omega_s t} + I_{s2}e^{-j\omega_s t})^{*}\right\} \quad (18)$$

$$Q_s = \frac{3}{2}\mathrm{Im}\left\{\vec{v_s}.\vec{i_s}^{*}\right\} = 3\mathrm{Im}\left\{(V_1e^{j\omega_s t} + V_2e^{-j\omega_s t}).(I_{s1}e^{j\omega_s t} + I_{s2}e^{-j\omega_s t})^{*}\right\} \quad (19)$$

Which yields:

$$P_s = 3\mathrm{Re}\left\{V_1I_{s1}^{*} + V_1I_{s2}^{*}e^{j2\omega_s t} + V_2I_{s1}^{*}e^{-j2\omega_s t} + V_2I_{s2}^{*}\right\} \quad (20)$$

$$Q_s = 3\mathrm{Im}\left\{V_1I_{s1}^{*} + V_1I_{s2}^{*}e^{j2\omega_s t} + V_2I_{s1}^{*}e^{-j2\omega_s t} + V_2I_{s2}^{*}\right\} \quad (21)$$

where subscripts 1 and 2 indicate positive and negative sequence components, respectively. ωs is the synchronous speed in rad/s. I_{s1} and I_{s2} are stator currents during positive and negative sequence components, respectively.

Having the aforementioned areas into consideration, the control loop with the inclusion of the negative sequence components for the given grid-tied DFIG under voltage dip conditions is designed and analyzed as it is unfolded in the next sections.

5. DUAL VECTOR CONTROL TECHNIQUES

The objective of this strategy is to reduce the stator overcurrents and as a consequence, the rotor overcurrents that appear in the DFIG windings during the sag using adapting the control of the RSC during this kind of event and without using any external crowbar circuit [26]. The most intuitive way to control a current vector, consisting of positive and negative sequence components is to use a current controller based on two synchronous reference frames, rotating at the fundamental grid frequency in the positive and the negative directions respectively as most of the unbalanced voltage problems can be overcome by introducing a precise amount of negative sequence components in the current references. In this way, the current references are becoming the addition of two sequences: one synchronized with the positive sequence of the grid voltage, and the other synchronized with the negative one [4, 26]. To guarantee that the two sequences are well regulated, it is necessary to independently control each sequence. The original control loop is then substituted by two control loops, one working in a positive rotating reference frame and the other working in an inversely rotating reference frame [22]. This is why the strategy called the dual vector control technique is used in dip periods.

6. CROWBAR AND ITS DESIGN

In addition to developing a control system for the protection of a WT during grid faults, a crowbar circuit can be designed as a control system for positive and negative sequence components of the fault current. In a practical wind power plant, the crowbar is a commonly used practice for the protection of the generator and convertor. The crowbar is

implemented by short-circuiting a low resistance across the rotor windings [27]. As a result, a large amount of current is produced and is allowed to flow via the resistor circuit instead of flowing in the RSC. The dynamic behavior of the power system during a dip phenomenon is greatly affected by the resistor value of the crowbar. For this reason, the crowbar resistors should be sufficiently low to avoid large voltages on the converter terminals. On the other hand, it should be high enough to limit the rotor current. Thus, the resistance of the crowbar R_{crow} must be chosen carefully. In [27], they chose the resistance value to be equal to 30 R_r, where R_r is the rotor resistance of DFIG.

7. RESULTS AND ANALYSIS

7.1. Comparison of Gradual Voltage Reduction Based on Experiments and Sudden Voltage Drops

A 5 kW DFIM whose parameters are obtained as in [28] is used with its setup shown in Fig. 1 and tested in the laboratory for gradual voltage reduction at real-time operation for rated voltage (400 V, LL), and a reduced voltage of 300 V, LL and 200 V, LL using a microcontroller of the Texas Instrument's (TI) under the application of a Code Composer Studio Software (CCS) to be compared with sudden voltage dip as the results are shown in Fig. 2. Due to the lack of a programmable voltage source in the laboratory, it was not possible to make experimentation on sudden voltage dips. The analysis and simulations were conducted in the Matlab/Simulink user-defined function toolbox. However, the machine has no inbuilt MATLAB and controllers. External PWM modulation inverter, the DC link system, current and voltage probes, variable power supply as a grid voltage, microcontroller with Texas Instrument CCS software, and others have been used as shown in Fig. 2. The DFIM is driven by the emulator induction motor as shown in Fig. 2 and not driven by a real wind turbine. Moreover, the speed is not fixed, it is variable to show the varying nature of the wind speed.

Fig. 2. DFIM under experimentation with associated accessories.

As can be seen from the experimental results (shown in Fig. 3) at voltages of 400 V, 300 V, and 200 V, a gradual reduction of stator voltage has the same effects of reduction on the stator and rotor currents. In addition, the results can clearly show the ability of dq rotor current references in controlling the stator and rotor active and reactive powers by applying CCS software in a microcontroller of Texas Instruments.

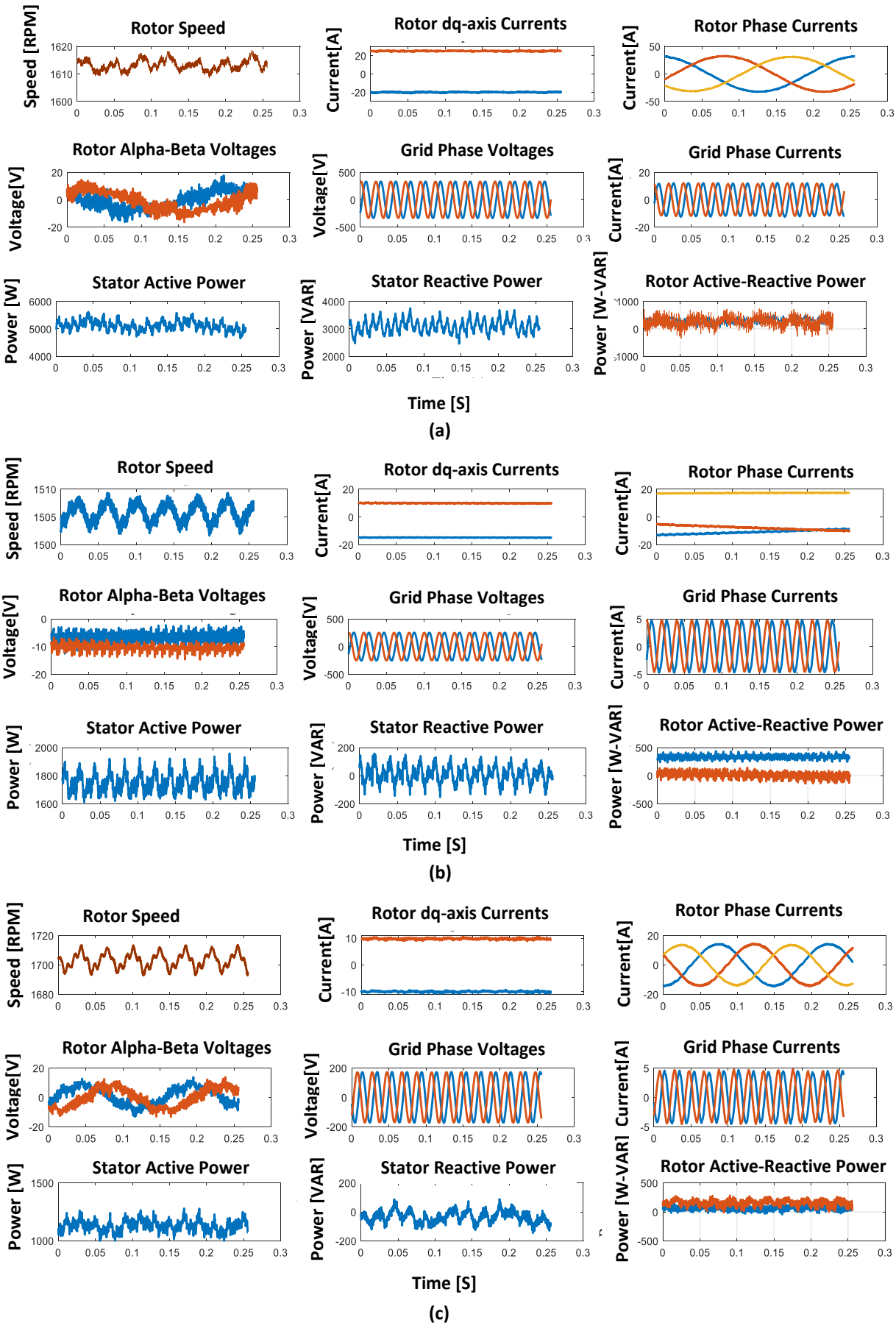

Fig. 3. Experimental results at different voltages: a) 400 V, LL rms; b) 300V, LL rms; c) 200 V, LL rms.

It can be noted that a sudden voltage drops (dip) as seen in Fig. 4 has quite different effects compared with a gradual reduction of the stator voltages in Fig. 3. As a result, a sudden drop in the stator voltages has a huge impact on the increments of stator and rotor currents affecting the machine's performance. This can be one of the main concerns towards voltage dip analysis of the DFIG in grid-tied WECS.

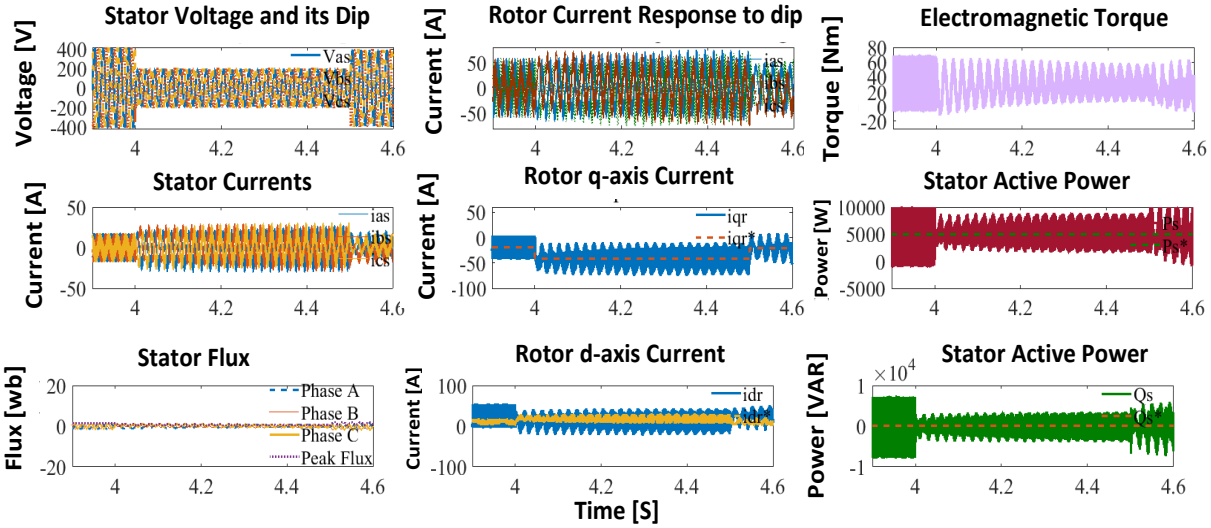

Fig. 4. Simulation results for sudden voltage dip from 400V to 200V.

7.2. Simulation Results

This part analyzes a symmetrical voltage dip carried out on a 5 kW DFIM whose model is done in MATLAB/Simulink/PowerSym as shown in Fig. 5. The analysis is carried out first without and then with crowbar activation accompanied by a vector control towards grid codes.

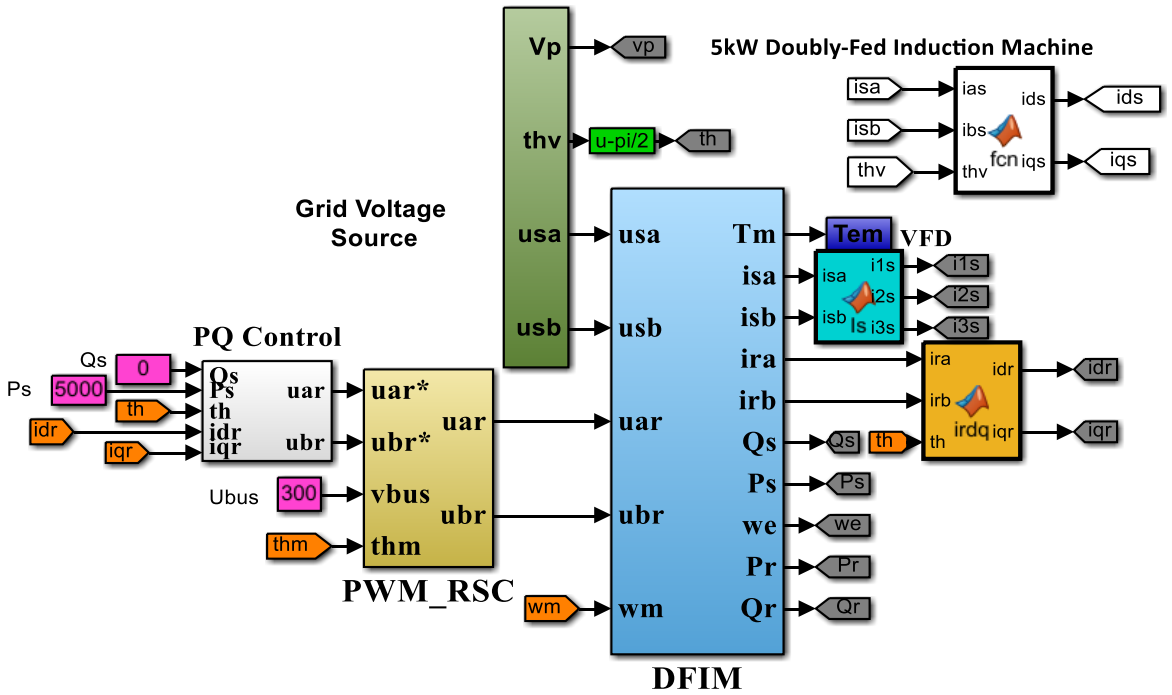

Fig. 5. DFIG Model in MATLAB-Simulink for voltage dip analysis.

7.2.1. Without Crowbar

The performance of the DFIG under a balanced three-phase of 90 % voltage dip occurred at a time between t = 4 - 4.5 s is shown in Figs. 6 and 7 with no crowbar activation.

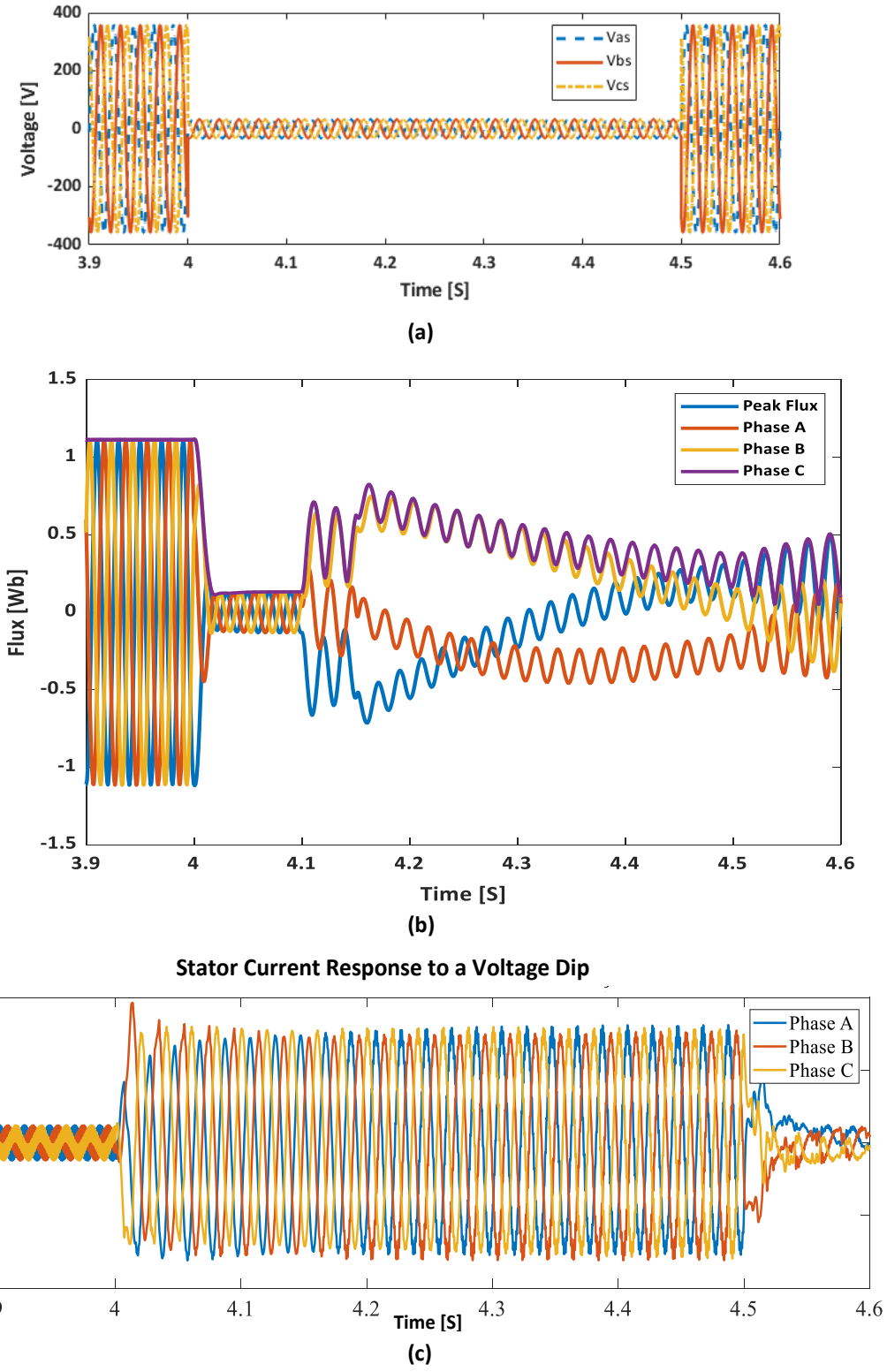

Fig. 6. Flux and stator current responses to a 90% symmetrical voltage dip: a) grid voltage dip of 90%; b) stator flux evolution during a 90 % voltage dip; c) stator current response to a voltage dip.

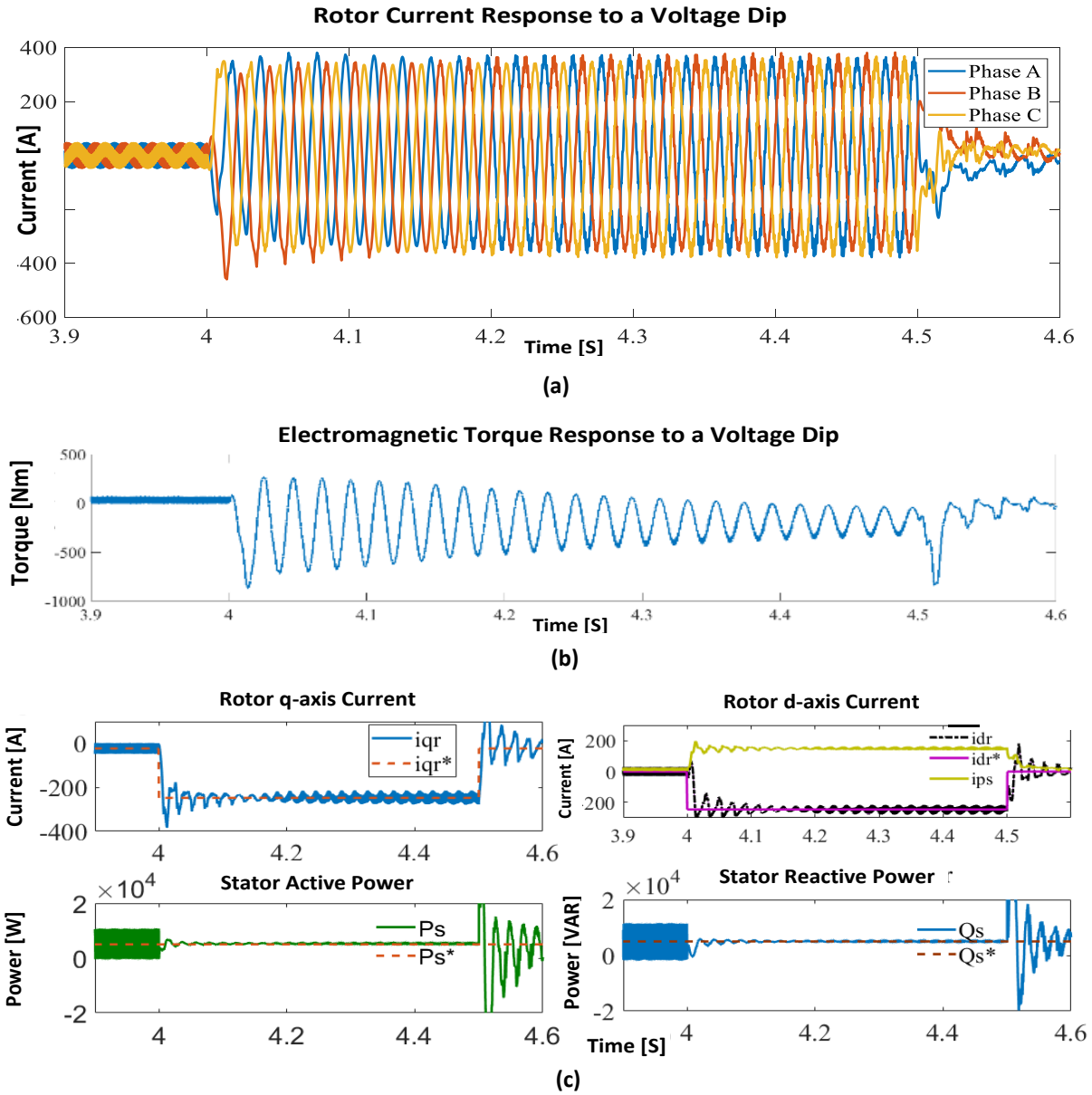

Fig. 7. A 90% symmetrical voltage dip and generated power responses: a) rotor current response to a voltage dip; b) electromagnetic torque for the applied voltage dip; c) current control loops during a voltage dip.

As can be seen from the above simulation results, during the steady-state operation, the stator flux is proportional to the stator voltage (Figs. 6(a) and (b)). However, this situation is changing during voltage dip conditions and as a result, therefore, the machine will demagnetize slowly for deeper voltages like the above one.

When a sudden voltage dip occurs at the terminals of the DFIM, the stator flux cannot evolve to its final steady state as quickly as its voltage [13]. This is shown in Fig. 6(b) for the given machine under study with no crowbar activation.

In real-time practical systems like WECS, perfect conditions for the analysis of characteristics harmonics which is another class of power quality problems of converters, never met [29]. However, when the crowbar is activated by letting all the rotor current flow through it, the current can then make the flux decay more quickly as shown in Fig. 8(c). This can be a good implication for the importance of using a crowbar activation during a voltage dip phenomenon.

It is seen again that, once the fault occurs at t = 4 s, there is a huge amount of rotor current which is almost more than four times the rated current as seen in Fig. 7(a). This current will lead to damage the power converter in the rotor unless some kind of protection and /or control techniques are not applied and the converter is not oversized.

The strongest voltage dip (90 %) is considered in this case as it resulted in a higher induced emf and larger rotor and stator currents as shown in Fig. 6(c) and Fig. 7(a). Thus, the implementation of a well-developed control system with some kind of protective equipment, such as a crowbar becomes compulsory. The rotor speed has also an influence on the current as the induced emf is proportional to it. In this case, the machine is running at a constant super-synchronous speed (1800 rpm).

7.2.2. With Crowbar Activation

The increased rotor current can be reduced by the implementation and activation of a crowbar circuit for a voltage dip with progress recovery as shown in Fig. 8(a) and its rotor current response as shown in Fig. 8(b).

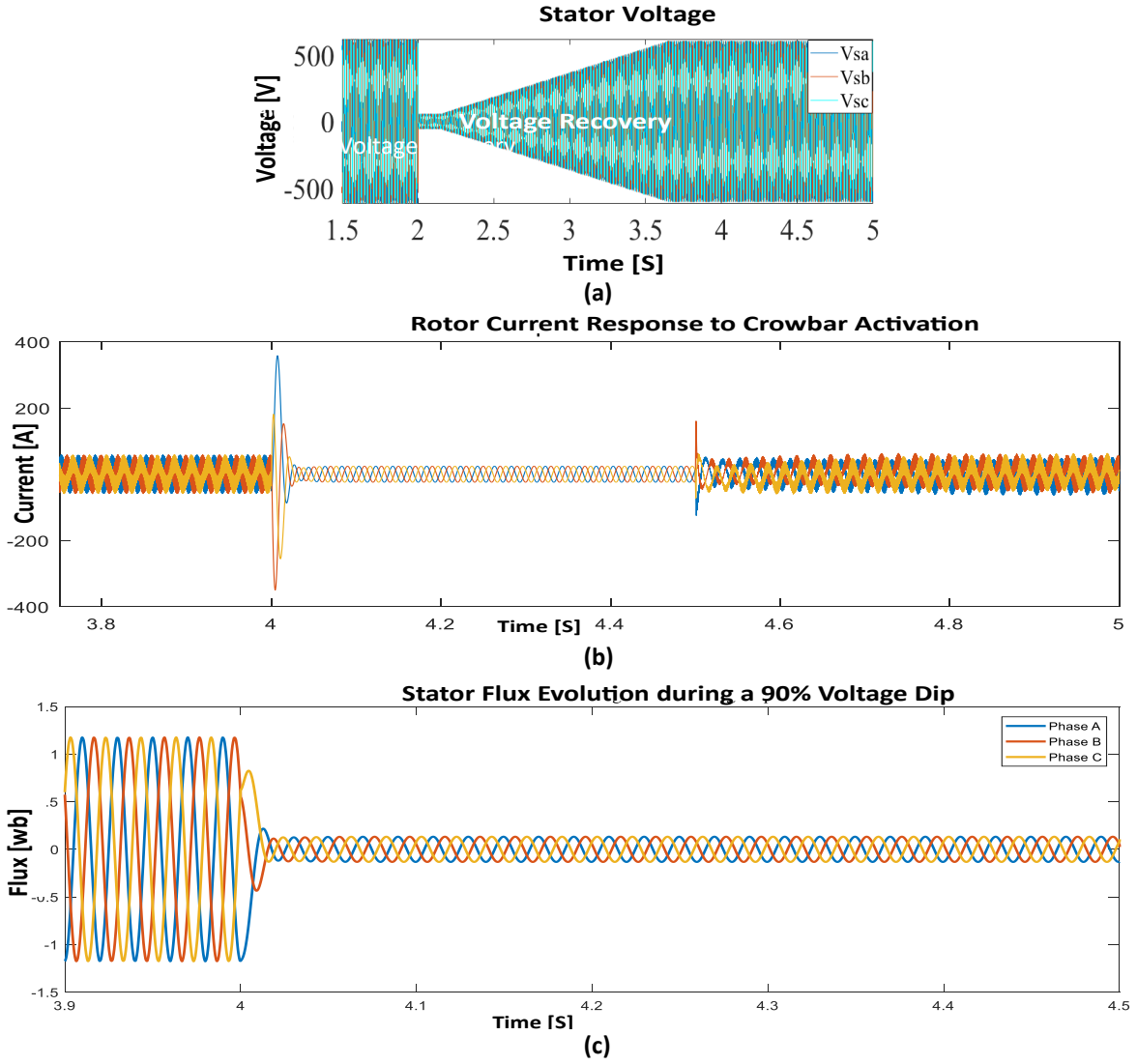

Fig. 8. Simulation results for rotor current and stator flux responses with crowbar activation: a) voltage dip and its recovery; b) rotor current response to a crowbar activation during a 90 % dip; c) stator flux evolution for a 90 % voltage dip with crowbar activation.

In the simulation results, the crowbar is activated at t = 4s immediately after the occurrence of a voltage dip by letting all currents flow through it as shown in Fig. 9(a), and disappears at 4.5 s. At times between t = 4.5 s - 5 s, the voltage recovery starts, and the machine returns to its normal operation (Fig. 8(a)) following the same pattern of the grid code requirements of the German power system operator [30].

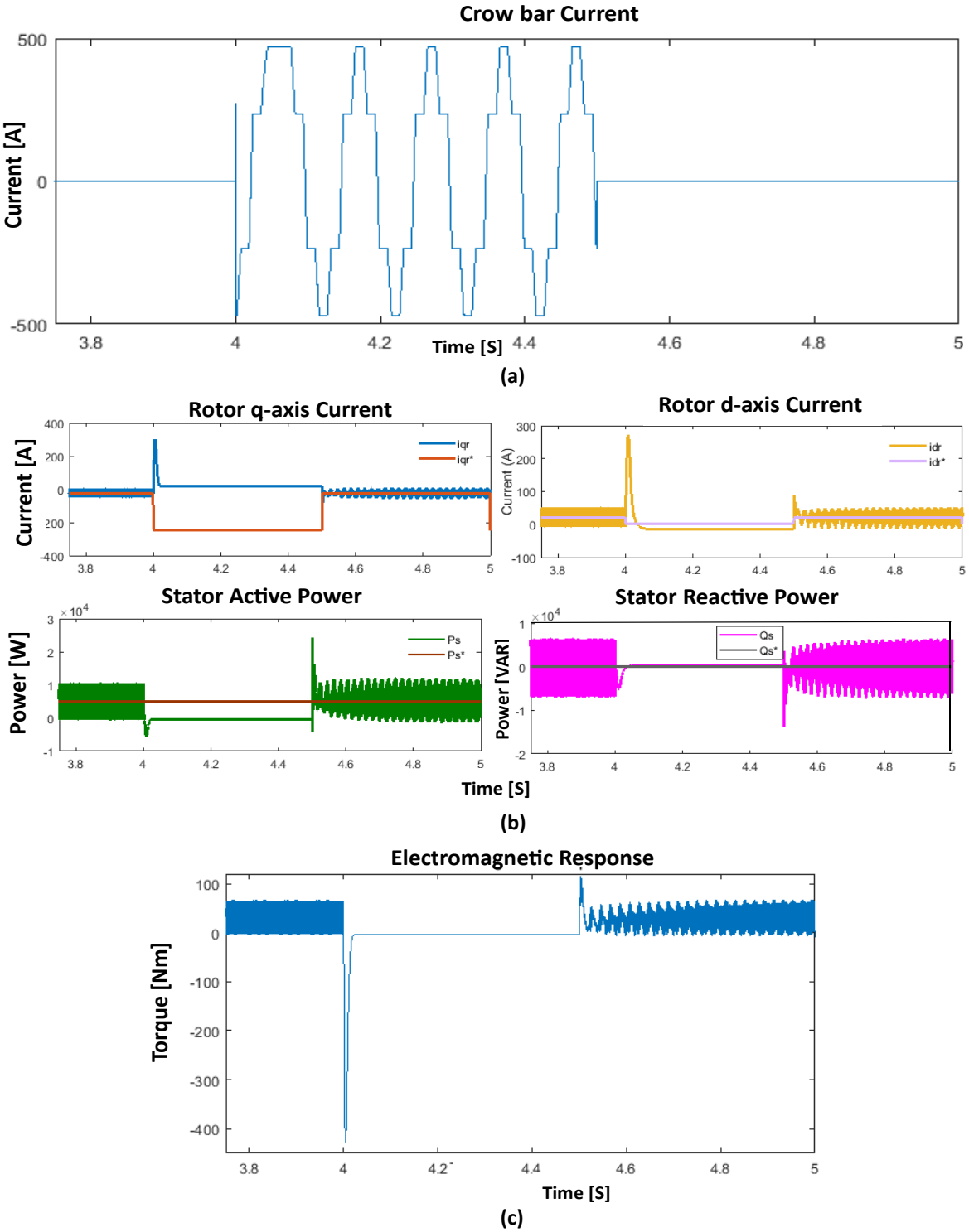

Fig. 9. Simulation results for voltage dip of 90 % with crowbar activation: a) current through a crowbar during a voltage dip of 90%; b) stator active and reactive power tracking with rotor quadrature axis reference (iqr*) and rotor direct axis reference (idr*) during a voltage dip of 90%; c) electromagnetic torque response.

During these periods (4 - 4.5 s), the rotor current tends to zero (Fig. 8(b)). Consequently, the q (i_{qr}) and d-axis (i_{dr}) rotor currents which are used to control the active and reactive power respectively respond accordingly. Initially, in this simulation, the active power is controlled to produce the rated power (5 kW) and the reactive power to zero for unity power factor operation.

As a result, the reference currents are tracking their respective currents during normal operation periods (Fig. 9(b)) as fulfilling the objective of the task. As of a closed loop nature, the change in the actual rotor current during a voltage dip is reflected in its reference one. Accordingly, the PI controller is tuning to adjust the change to a new set value, and hence the rotor current decreases to zero for the whole period of fault as shown in Figs. 8(b) and 9(b).

It can be seen from the above simulation results that the control of active and reactive power is lost during a crowbar activation for a given voltage dip. In addition, the electromagnetic torque control (shown in Fig. 9(c)) is also lost, which is a risky condition in a real grid-tied wind power system. Therefore, it is the main concern to support the grid with reactive power demand with no/minimum active power generation using the control techniques during a voltage dip and crowbar activation period as seen by simulation results.

8. GRID CODE REQUIREMENT AND ITS FULFILLMENT

As per the latest grid codes of various countries, wind turbines (WTs) are required to inject some amount of reactive and active current into the faulty grid during voltage dips [21, 31].

Over the past years, the grid codes have toughened their requirements, demanding each year a quicker injection of reactive current that is why this paper is focused on the control of the reactive power injection to the grid during voltage dip by limiting the active power generation through the stator.

As explained earlier, the DFIG is not supposed to disconnect from the power grid during voltage dip conditions, rather they are expected to support the grid via reactive power as per the recent grid code requirements. This can be achieved through well-controlled mechanisms by changing the rotor reference current controllers. Thus, in this case, a control strategy is implemented in such a way that the rotor d-axis current has to track the peak currents of the stator of the machine to support the grid with the reactive power, and a q-axis component of the rotor is made to zero for no active power production during a dip period as the results show in Fig. 10.

In Fig. 10 simulation results, the periods between 0-4 s and 5-6 s are normal or steady state operations whereas times between t = 4 - 4.5 s are voltage dips. The crowbar is activated at a time t = 4 s and deactivated at 4.1 s operating for 100 ms.

At times between 4.15 - 4.50 s, the d-axis controller (i_{dr}*) is adjusted equivalent to the peak value of the stator peak current (i_{ps}) to fulfill grid code requirements by supporting the grid with reactive power and no active power production during that period. As a result, the control activity can make the DFIG supply reactive power to the weak grid, which will increase and help its voltage recovery and ensure stability.

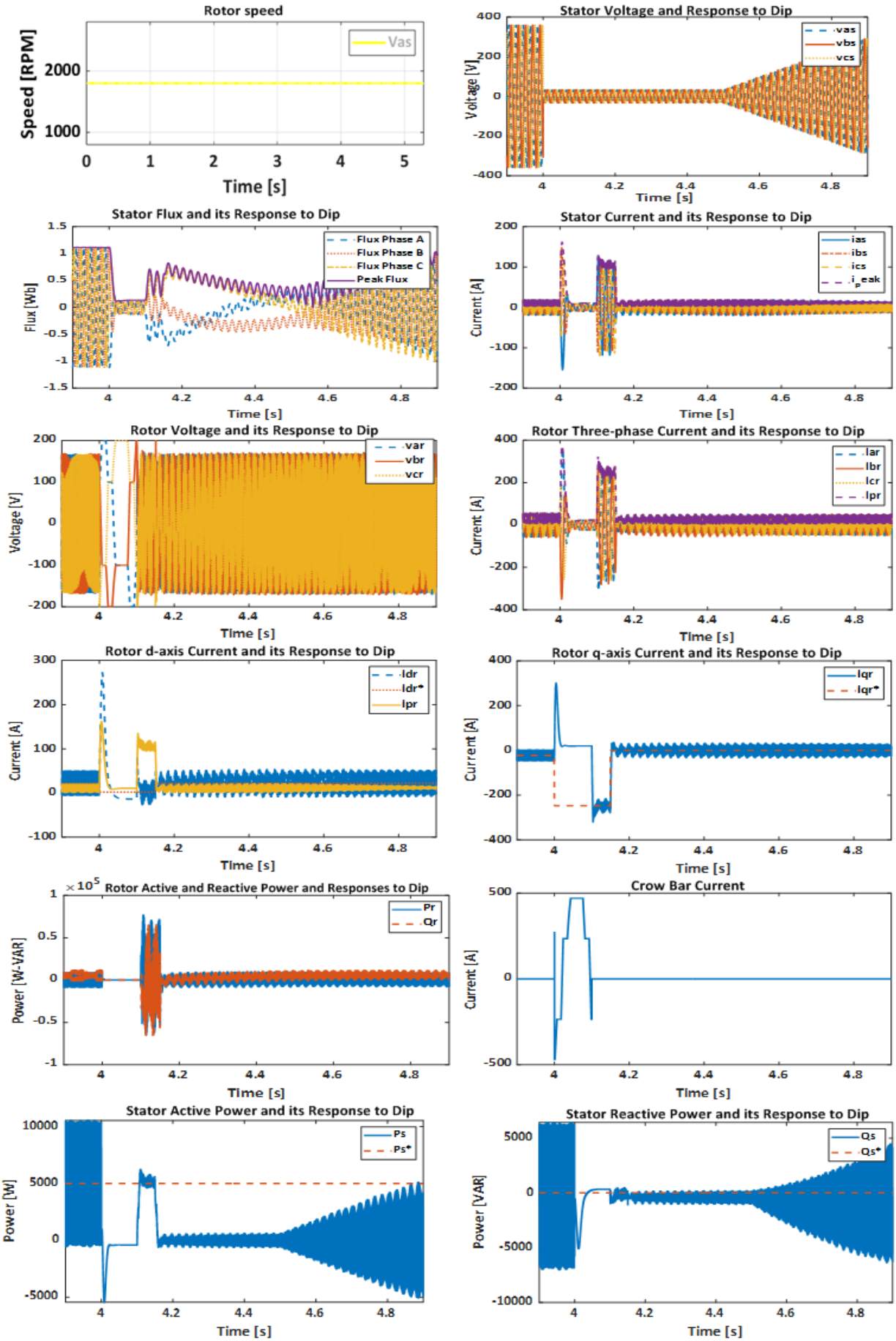

Fig. 10. Results of 90 % voltage dip and supporting the grid with reactive power.

The basic vector control scheme is introduced into the rotor current of the given DFIG to generate the desired stator powers on the equations obtained [5]:

$$i_{qr}^{*} = -\frac{2}{3}\frac{L_s}{L_m}\frac{1}{V_{fault}}P_s \; ; \; i_{dr}^{*} = -\frac{2}{3}\frac{L_s}{L_m}\frac{1}{V_{fault}}Q_s + \frac{V_{fault}}{\omega_s L_m} \quad (22)$$

where L_s and L_m are the self-inductance of the stator and mutual inductance (H), respectively.

Based on Eq. (22), for instance, to produce -1 kVAR reactive power for a voltage dip of 90% on a given DFIG, i_{dr}^{*} = 21.9 A [zoomed] as shown in Fig. 8 is required and 43 A to produce -2 kVAR where V_{fault} = 0.1*V_{LL}, RMS = 0.1*326.6 V = 32.66 V.

This implies that a given DFIG under study cannot support the grid with more than 1 kVAR without surpassing the RMS limit of the rotor current at 90 % voltage dips. However, the amount varies for varying voltage dips. The maximum rotor current of the machine under study is 21 A [28]. By setting the reference of the rotor current to this value (21.9 A) at a time t = 4.15 s after a crowbar is deactivated at 4.1 s, the rotor voltage is decreased simultaneously and we can obtain the desired powers as per the grid codes. Even though these extra powers are oscillating, the peak value reaches the desired powers. In periods between t = 4.1 - 4.15 s, the controller is tuned to track for P_s = 5 kW and Q_s = 0 which is the same as during the steady-state operation.

On the other hand, for a shallower dip, for instance, a 10 % dip, i_{dr}^{*} = 19.2 A can generate near -5 kVAR reactive power to the grid without exceeding the rated rotor current.

From the above analysis, it is possible to control the active and reactive power to any value as per any of the grid code requirements. Moreover, the simulation results can confirm that the LVRT operation of the DFIG with the proposed protection strategy for a voltage dip of 90 % works well.

Therefore, it can be summarized in such a way that, a symmetrical voltage dip for longer periods is very challenging to control the desired parameters without disconnecting WT from the grid and without surpassing the reference points. For shorter periods, the control system developed for the given machine performs very fine for RSC and GSCs. In addition, the authors recommend the use of a crowbar with a well-developed control strategy for stable operation and better protection of the converter unless and otherwise the oversized converter is used in its design.

9. CONCLUSIONS

In this paper, a voltage dip analysis of a 5 kW DFIG supported by laboratory test results is carried out. The voltage dip which happens suddenly in a certain power network results in quite different nature as of gradual voltage decreases and hence needs strong attention.

In this paper, a laboratory test was carried out with the lack of a programmable power supply, and hence its use can be recommended for further research works to validate the results. In addition, asymmetrical voltage dips are not in-depth dealt with in this paper and also be another area of recommendation.

Finally, the paper determined the amount of reactive power to support the grid under a severe 90 % voltage dip and shallower 10 % dips. The results show that the given DFIG

cannot support the grid with more than 1 kVAR without violating the RMS limit of the rotor current at 90 % voltage dips. The work can be extended for various kinds of voltage dips happening at the grid side of the wind energy conversion system.

Acknowledgment: The author has received research support from German Academic Exchange Service (DAAD) and highly acknowledges it.

REFERENCES

[1] T. Ackermann, *Wind Power in Power Systems*, 2nd Edition, John Wiley and Sons, 2012.

[2] C. Shiva, Vigya, B. Vedik, R. Kumar, S. Rangarajan, V. Mukherjee, "Analysis of voltage sag in DFIG based wind power system," *AIP Conference Proceedings*, vol. 2418, no. 1, pp. 40005, 2022.

[3] R. Teodorescu, M. Liserre, P. Rodríguez, *Grid Converters for Photovoltaic and Wind Power System*, John Wiley and Sons, 2011.

[4] G. Abad, J. Lopez, M. Rodriguez, L. Marroyo, G. Iwanski, *Doubly Fed Induction Machine: Modeling and Control for Wind Energy Generation*, 1st Edition, IEEE and John Wiley and Sons, 2011.

[5] Y. Pavan Kumar, L. Kumar, D. Ananth, C. Reddy, A. Flah, H. Kraiem, J. Al-Asad, H. Kotb, K. Aboras, "Performance enhancement of doubly fed induction generator–based wind farms with STATCOM in faulty HVDC grids," *Frontiers in Energy Research*, vol. 10, pp. 930268, 2022.

[6] F. Blaabjerg, Z. Chen, *Power Electronics for Modern Wind Turbines*, 1st edition, Morgan and Claypool, USA, 2006.

[7] S. Mohamed, "A novel precise steps-based independent active and reactive power flow controller," *Jordan Journal of Electrical Engineering*, vol. 4, no. 3, pp. 129-142, 2018.

[8] J. Dallachy, I. Tait, "Guidance note for the connection of wind farms," *SP Transmission and Distribution*, *Scottish Hydro-Electric*, 2002.

[9] O. Anaya-Lara, N. Jenkins, "Fault current contribution of DFIG wind turbines," *3rd International Conference on Reliability of Transmission and Distribution Networks,* London, pp. 75-79, 2005.

[10] G. Pannell, D. Atkinson, R. Kemsley, L. Holdsworth, P. Taylor, O. Moja, "DFIG control performance under fault conditions for offshore wind applications," *In CIRED 2005-18th International Conference and Exhibition on Electricity Distribution, Turin, Italy*, pp. 1-5, 2005.

[11] D. Xiang, L. Ran, P. Tavner, J. Bumby, "Control of a doubly fed induction generator to ride through grid fault," *International Conference of Electric Machines,* Cracow, Poland, 2004.

[12] J. Morren, S. De Haan, "Ride through of wind turbines with doubly fed induction generator during a voltage dip," *IEEE Transactions on Energy Conversion*, vol. 20, no. 2, pp. 435-441, 2005.

[13] N. Jouko, "Voltage dip ride-through of a double-fed generator equipped with an active crowbar," *Nordic Wind Power Conference, Chalmers University of Technology,* Gothenburg, Sweden, 2004.

[14] I. De Oliveira, F. Tofoli, V. Mendes, "Thermal analysis of power converters for DFIG-based wind energy conversion systems during voltage sags," *Energies*, vol. 15, no. 9, pp. 3152, 2022.

[15] N. Naidu, B. Singh, "Experimental implementation of a doubly fed induction generator used for voltage regulation at a remote location," *IEEE Transactions on Industry Applications*, vol. 52, no. 6, pp. 5065-5072, 2016.

[16] J. Abramowski, R. Posorski, "Wind energy for developing countries," *Dewi Magazine,* pp. 46-54, 2000.

[17] G. Bekele, A. Abdela, "Investigation of wind farm interaction with Ethiopian electric power corporation's grid," *Elsevier Energy Procedia,* vol. *14*, pp. 1766–1773, 2012.

[18] Renewables Now, *Ethiopian Wind Installed Capacity*, 2022. <https://renewablesnow.com /news/ethiopia-seeks-to-add-12-gw-of-windcapacity-starts-tender-529452/>

[19] B. Wu, M. Narimani, *High-Power Converters, and AC Drives*, 2nd edition, IEEE Press and John Wiley, New Jersey, USA, 2017.

[20] P. Krause, O. Wasynczuk, S. Sudhoff, S. Pekarek, *Analysis of Electric Machinery and Drive Systems*, 3rd Edition, IEEE Press and John Wiley, 2013.

[21] B. Hopfensperger, D. Atkinson, R. Lakin, "Stator-flux oriented control of a DFIM with and without position encoder," *Proceedings of IEEE Electric Power Applications*, vol. 147, no. 4, pp. 241-250, 2000.

[22] H. Abu-Rub, M. Malinowski, K. Al-Haddad, *Power Electronics for Renewable Energy Systems, Transportation and Industrial Applications*, First Edition, IEEE Press and John Wiley and Sons, United Kingdom, 2014.

[23] H. Huang, P. Ju, X. Pan, Y. Jin, X. Yuan, Y. Gao, "Phase–amplitude model for doubly fed induction generators," *Journal of Modern Power Systems and Clean Energy*, vol. 7, pp. 369-379, 2018.

[24] M. Tuka, "DC link voltage and power flow control of doubly fed induction generator in wind power system," *Proceedings of IEEE PES-IAS Power Africa*, pp. 1-5, 2020.

[25] G. Abad, *Power Electronics and Electric Drives for Traction Applications*, First Edition, Mondragon University, Spain, John Wiley and Sons, 2017.

[26] F. Lima, A. Luna, P. Rodriguez, E. Watanabe, F. Blaabjerg, "Rotor voltage dynamics in the doubly fed induction generator during grid faults," *IEEE Transactions on Power Electronics*, vol. 25, no. 1, pp. 118-130, 2010.

[27] S. Chandrasekaran, Grid Connected Doubly Fed Induction Generator-Based Wind Turbine Under LVRT, *Ph.D Dissertation*, Bologna, Italy, 2014.

[28] M. Berhanu, R. Leidhold, Z. Muluneh, Y. Mekonnen, A. Sarwat, "Real-time control of a doubly fed induction machine for variable speed constant frequency wind power system through laboratory test rig," *Proceedings of IEEE PES-IAS Power Africa*, pp. 195-201, 2018.

[29] H. Al-Majali, B. Al-Majali, "Control of AC/DC converter under unbalanced system conditions," *Jordan Journal of Electrical Engineering,* vol. 1, no. 1, pp. 25-36, 2015.

[30] M. Rahimi, M. Parniani, "Grid-fault ride-through analysis and control of wind turbines with doubly fed induction generators," *Electric Power Systems Research*, vol. 80, no. 2, pp.184-195, 2010.

[31] Z. Li, H. Xu, Z. Wang, Q. Yan, "Stability assessment and enhanced control of DFIG-based WTs during weak AC grid," *IEEE Access*, vol. 10, pp. 41371-41380, 2022.